

Preprint of

Optimal Control Design of Excitation Pulses that Accomodate Relaxation

N. I. Gershenzon, K. Kobzar, B. Luy, S. J. Glaser, T. E. Skinner

J. Magn. Reson. 188, 330-336 (2007).

Optimal control design of excitation pulses that accommodate relaxation

Naum I. Gershenzon^a, Kyryl Kobzar^b, Burkhard Luy^b,
Steffen J. Glaser^b Thomas E. Skinner^{a,*},

^a*Physics Department, Wright State University, Dayton, OH 45435, USA*

^b*Institut für Organische Chemie und Biochemie II, Technische Universität München, Lichtenbergstr. 4, 85747 Garching, Germany*

Abstract

An optimal control algorithm for mitigating the effects of T_1 and T_2 relaxation during the application of long pulses is derived. The methodology is applied to obtain broadband excitation that is not only tolerant to RF inhomogeneity typical of high resolution probes, but is relatively insensitive to relaxation effects for T_1 and T_2 equal to the pulse length. The utility of designing pulses to produce specific phase in the final magnetization is also presented. The results regarding relaxation and optimized phase are quite general, with many potential applications beyond the specific examples presented here.

Key words: RC-BEBOP; Relaxation; T_1 relaxation; T_2 relaxation; Optimal control theory

PACS:

1 Introduction

Optimal control theory has proven to be an extremely flexible and powerful tool for designing pulses for NMR spectroscopy. A particularly challenging problem, that of producing uniform excitation over a broad range of chemical shift offsets and RF field inhomogeneity/miscalibration, simultaneously, has been solved in a series of papers demonstrating Broadband Excitation by Optimized Pulses (BEBOP) [1–5]. The minimum pulse length of a given BEBOP

* Corresponding author.

Email addresses: glaser@ch.tum.de (Steffen J. Glaser),
thomas.skinner@wright.edu (Thomas E. Skinner).

depends upon the performance level required for the specific range of offset and RF variation accommodated [3], but it can significantly exceed the length of a hard pulse that would conventionally be used to excite the same bandwidth (albeit nonuniformly and with poor tolerance to RF inhomogeneity). So far, we have assumed that the longitudinal, T_1 , and transverse, T_2 , relaxation times are much larger than the duration of the pulse, which will not always be the case in practice. We therefore consider the design of BEBOPs that can [[**minimize relaxation effects**,]] or Relaxation Compensated-BEBOP.

The effect of relaxation on pulse performance has been studied in detail by Hajduk et al. [6]. When T_2 and/or T_1 are comparable to the pulse length, t_p , they not only found the expected loss of signal due to relaxation, but a significant degradation in uniformity of the excitation profile for all the pulses they considered. However, the literature on actual pulse design to mitigate the effects of relaxation appears to be relatively sparse and applied to narrowband, selective pulses. Nuzillard and Freeman modified BURP pulses to obtain more uniform response over the selected bandwidth with SLURP [7], but accepted what might be considered the inevitable attenuation due to short T_1 , T_2 . Rourke et al. [8] later developed an iterative method for designing selective pulses to compensate for transverse relaxation. The procedure they presented did not accommodate either T_1 effects or RF inhomogeneity. They obtained a significant improvement in the uniformity of pulse response, but actual T_2 losses were not provided, and the method assumes $1/T_2$ is small [9]. Reference [9] derives a method for inverting the Bloch equation at a single resonance offset for the special case $T_1 = T_2$. Its primary application is to pulses which select a specific relaxation rate, which is different than what we are considering here.

Expanding on these earlier works, we explore more generally the possibilities for reducing [[**DELETE: or eliminating**]] relaxation effects during long RF pulses (ie., relative to T_2 and/or T_1). Optimal control can consider both T_1 and T_2 relaxation together with RF inhomogeneity over any specified range of offsets, either connected or disjoint. Moreover, there is a physical basis for expecting to be able to compensate for relaxation during the pulse: we can i) use the long duration of the pulse to position spins of different chemical shift at appropriate orientations near the z axis that enable them to be subsequently transformed to the x, y plane by a short pulse segment, reducing net T_2 relaxation during the total pulse and ii) utilize the moderate, but still significant, repolarization that occurs for short T_1 . These possibilities for reducing relaxation effects are found quite naturally by the optimal control algorithm, as shown in what follows. There does not appear to be any other study which attempts to reduce the effects of relaxation in pulses of length similar to T_1 , T_2 .

2 Theory and Methods

Optimal control theory applied to NMR spectroscopy has been described in detail elsewhere [1–5,10–12], for systems with no relaxation (ie., infinite T_1, T_2). Here we reiterate the main theoretical aspects and introduce the necessary modifications associated with finite T_1, T_2 .

During the time interval $[t_0, t_p]$, we seek to transfer initial z magnetization $\mathbf{M}(t_0)$ for a system of non-interacting spins to a desired final state \mathbf{F} over a given range of chemical shift offsets $\Delta\omega$ and RF field inhomogeneity/miscalibration for specified values of T_1 and T_2 . The spin trajectories $\mathbf{M}(t)$ are constrained by the Bloch equation

$$\dot{\mathbf{M}}(t) = \boldsymbol{\omega}_e(t) \times \mathbf{M}(t) + D[\mathbf{M}_0 - \mathbf{M}(t)], \quad (1)$$

where $\mathbf{M}_0 = \hat{\mathbf{z}}$ is the unit equilibrium polarization for appropriately normalized units, the effective field, $\boldsymbol{\omega}_e$, in angular frequency units (rad/s) is given in terms of the time-dependent RF amplitude, ω_1 , and phase, ϕ , as

$$\begin{aligned} \boldsymbol{\omega}_e(t) &= \omega_1(t) [\cos \phi(t) \hat{\mathbf{x}} + \sin \phi(t) \hat{\mathbf{y}}] + \Delta\omega \hat{\mathbf{z}} \\ &= \boldsymbol{\omega}_{rf}(t) + \Delta\omega \hat{\mathbf{z}}, \end{aligned} \quad (2)$$

and the relaxation matrix is

$$D = \begin{pmatrix} 1/T_2 & 0 & 0 \\ 0 & 1/T_2 & 0 \\ 0 & 0 & 1/T_1 \end{pmatrix}. \quad (3)$$

Proceeding as in our previous treatments, a time-dependent ‘‘hamiltonian’’ h is defined in terms of a Lagrange multiplier $\boldsymbol{\lambda}$ as

$$h(t) = \boldsymbol{\lambda}(t) \cdot \dot{\mathbf{M}}(t) = \boldsymbol{\lambda} \cdot [\boldsymbol{\omega}_e \times \mathbf{M} + D(\mathbf{M}_0 - \mathbf{M})], \quad (4)$$

which returns the Bloch equation as

$$\dot{\mathbf{M}} = \partial h / \partial \boldsymbol{\lambda} \quad (5)$$

with the known value $\mathbf{M}(t_0)$ at the beginning of the pulse. For a given cost function Φ chosen to measure pulse performance, the optimization formalism results in the conjugate or adjoint equation

$$\dot{\boldsymbol{\lambda}}(t) = -\partial h / \partial \mathbf{M} \quad (6)$$

$$= \boldsymbol{\omega}_e(t) \times \boldsymbol{\lambda}(t) + D \boldsymbol{\lambda}(t) \quad (7)$$

with the value $\boldsymbol{\lambda}(t_p) = \partial \Phi / \partial \mathbf{M}$ required at the end of the pulse, giving $\boldsymbol{\lambda}(t_p) = \mathbf{F}$ for the cost

$$\Phi = \mathbf{M}(t_p) \cdot \mathbf{F}, \quad (8)$$

for example. In contrast to our earlier treatments without relaxation, $\boldsymbol{\lambda}(t)$ is governed by a different evolution equation than $\mathbf{M}(t)$. This is a result of the equilibrium polarization \mathbf{M}_0 in Eq. [1]. **[[In applications governed by a similar evolution equation, but absent the \mathbf{M}_0 term (for example, mixing pulses with relaxation [13,14]), the evolution of $\boldsymbol{\lambda}$ and \mathbf{M} differ only in the sign of the relaxation term, D .]]**

The final necessary condition that must be satisfied by a pulse that optimizes the cost function is

$$\partial h(t) / \partial \boldsymbol{\omega}_e(t) = 0 = \mathbf{M}(t) \times \boldsymbol{\lambda}(t) \quad (9)$$

at each time. For a nonoptimal pulse, Eq. [9] is not **[[fulfilled]]**. It then represents a gradient giving the proportional adjustment to make in the controls, $\boldsymbol{\omega}_e(t)$, for the next iteration towards an optimal solution. Additional constraints on the maximum allowed RF amplitude, ω_{\max} , may include clipping, $\omega_{\text{rf}}(t) \leq \omega_{\max}$, or pinning, $\omega_{\text{rf}}(t) = \omega_{\max}$.

The numerical algorithm has been described previously [1–5]. The addition of relaxation to the Bloch equation is the only modification. For excitation, the choice $\mathbf{F} = \hat{\mathbf{x}}$ produces a pulse with the specified tolerance to RF inhomogeneity which drives all spins in the range of offsets considered to the x axis. The resulting spectrum therefore requires no phase correction. However, this imposes a very stringent requirement on the optimal control algorithm.

A linear phase dispersion in the final magnetization as a function of offset is readily corrected in many practical applications and might allow more flexibility in optimizing the pulse. We therefore also introduce a target *function*

$$\mathbf{F} = \cos \varphi \hat{\mathbf{x}} + \sin \varphi \hat{\mathbf{y}} \quad (10)$$

where φ is defined as a linear function of $\Delta\omega$ and gives the angle between the final transverse magnetization at offset $\Delta\omega$ and the x axis. We have previously argued [5] that hard 90° pulses could be considered the benchmark for broadband performance in sequences that are readily phase-corrected. In

addition, hard pulses are likely the only option, currently, for broadband excitation if relaxation effects are important. We therefore choose the slope of $\varphi(\Delta\omega)$ to be that of a hard pulse with the same ω_{\max} as the optimized pulse under consideration.

3 Results and Discussion

We recently presented a purely phase-modulated BEBOP that provides an unprecedented combination of excitation bandwidth and tolerance to RF inhomogeneity. This PM-BEBOP gives uniform excitation of greater than 99% over the entire 200 ppm ^{13}C chemical-shift range of a potential 1 GHz spectrometer, for a constant RF amplitude anywhere in range 10–20 kHz [5]. However, the shortest pulse that achieves this level of performance is 1 ms, which could be problematic for applications with short T_2 and/or T_1 .

The loss of signal and distortion of the excitation profile that occurs when relaxation times are comparable to pulse length are illustrated in Fig. 1 for PM-BEBOP, operated at the ideally calibrated maximum RF of 15 kHz. The results are applicable to pulses in general when relaxation is a factor. For $T_2 = 1$ ms, PM-BEBOP suffers a minimum 50–60% signal loss for any **[[allowed]]** value of T_1 , and, as expected, the excitation is no longer uniform over the offset range. If T_2 is 5 times longer, this pulse still suffers a 15–20% signal loss compared to the ideal case of infinite T_2 .

Signal loss is reduced significantly, however, by incorporating relaxation into the optimal control algorithm. For comparison, we designed relaxation compensated pulses (RC-BEBOP) with a $\pm 5\%$ tolerance to RF inhomogeneity (typical high resolution probes) and the same PM-BEBOP excitation bandwidth of 50 kHz, optimized for the T_1 , T_2 combinations listed in the legend to Fig. 1. For $T_2 = 1$ ms, RC-BEBOP excites 90–95% of the target M_x magnetization for any T_1 , with excitation of at least 97% for $T_2 = 5$ ms.

By contrast, a hard pulse of the same 15 kHz amplitude ($t_{90} = 16.7\mu\text{s}$) is unaffected by a 1 ms T_1 and T_2 , giving slightly greater signal near resonance than RC-BEBOP, as shown in Fig. 2. However, the excitation profile is “parabolic,” with signal amplitude decreasing steeply with offset, so RC-BEBOP is a far better solution for broadband excitation in the presence of relaxation than a hard pulse of equivalent RF amplitude. Moreover, if we allow the optimal control algorithm to generate the same linear phase dispersion in the final magnetization that occurs for a hard pulse (eg., the target function of Eq. [10]), performance is improved even more dramatically. For the demanding case $T_1 = T_2 = t_p = 1$ ms, this additional RC-BEBOP uniformly excites 98–99% of the transverse magnetization over the entire offset range,

with linear phase, giving only a small signal loss of 1–2% compared to the case of PM-BEBOP with no relaxation.

One might expect a shorter pulse optimized without relaxation to be an alternative solution to the 1 ms RC-BEBOP considered. For example, in the absence of significant relaxation, a 125 μs BEBOP [4] designed with $\pm 5\%$ tolerance to RF inhomogeneity gives uniform excitation of 98% over an offset range of 40 kHz with phase deviations from the x -axis of less than 2° . Although t_p is an order of magnitude less than a 1 ms T_1 and T_2 , we still find significant distortion in the excitation profile if relaxation is included in the simulation. In this case, values of M_x for the ideally calibrated RF range from 0.95 to 0.88 over the bandwidth. **[[For further comparison, a phase-alternated composite excitation pulse [15] with the largest bandwidth (36 kHz for a 15 kHz amplitude) is 215 μs long and only excites 75–85% of the magnetization over the bandwidth when relaxation effects are included. Similar performance in the presence of relaxation is obtained for broadband polychromatic pulses [16].]]** Uniform excitation with reduced signal loss in the presence of relaxation is not necessarily achieved simply by using a shorter pulse.

The gain in signal that RC-BEBOP achieves over the uncompensated PM-BEBOP for short T_1 , T_2 is obtained by finding trajectories that not only transform magnetization to the desired target state, but keep the magnetization close to the z axis for as long as possible during the pulse. This is done concurrently for all spins in the optimized range of resonance offsets and RF inhomogeneity. An example for the ideal RF calibration is provided in Fig. 3, showing the relatively small changes that occur in spin orientation for each offset at progressively larger times during the pulse. The outer edges of the bandwidth require the most manipulation during the early stages of the pulse, with the bulk of the magnetization transformed to the transverse plane during the final 2% of the pulse.

An example illustrating the trajectories at several offsets during the pulse is provided in Fig. 4 for the linear target function used in Fig. 2 for the case $T_2 = 1 \text{ ms} = t_p$. The early part of the pulse is used to “stall” the spins near the z axis and orient them properly so they can all be transformed to the target state by an effectively shorter pulse at the end.

This mechanism is further illustrated by the pulse itself, shown in Fig. 5. There are only minor manipulations of the spins during the first 90% or so of the pulse. After $0.98T_p$, the spins are positioned so they can be transformed to the transverse plane by a simple hard pulse. The y -amplitude of the pulse is reminiscent of polychromatic pulses [16], which are purely amplitude modulated. The small x -amplitude modulation of RC-BEBOP only affects the extreme limits of the bandwidth significantly (the outer 10%). Effects of the

small RF oscillations during the first half of the pulse are demonstrable over the entire bandwidth at a numerical level, acting to smooth deviations from uniformity in the excitation profile. However, these deviations are significantly less than 1% and would be difficult to detect in an NMR experiment. Hence, a shorter 0.5 ms pulse starting in the middle of the 1 ms pulse shown would perform as well over 45 kHz bandwidth as the full pulse over 50 kHz.

As T_2 becomes shorter, it will still require the same amount of time to orient all the spins appropriately, so the quality factor measuring pulse performance will decrease with decreasing T_2 . Nonetheless, there are significant signal gains available using RC-BEBOP compared to an uncompensated pulse, as shown in Fig. 6, which compares quality factor as a function of T_2 for PM-BEBOP and RC-BEBOP. In addition, the calculations plotted in the figure confirm that there is an advantage to shorter T_1 , as suggested in the Introduction. For BEBOP in general, where the only constraint is to find spin-trajectories that arrive at the target, performance is degraded as T_1 decreases. When relaxation is added as a constraint, RC-BEBOP utilizes trajectories close to the z axis to not only reduce T_2 effects, but to increase signal due to T_1 repolarization of z -magnetization—the shortest possible T_1 will have the best performance in this scenario.

Thus, the length of the pulse doesn't matter after a certain point. Once a relaxation-compensated pulse of minimum length is found that maximizes performance for a particular application, optimizing with a longer pulse has the obvious solution of zero RF amplitude at the beginning followed by the minimum length pulse, giving the same performance. Figure 7 shows how the performance of RC-BEBOP depends on pulse length for values of T_1 between 1 ms and infinity for the specific choice of $T_2 = 1$ ms. The results reiterate the advantage of shorter T_1 when optimizing pulse performance to include relaxation. The effect is more pronounced only for T_1 shorter than considered in the figure.

The performance of RC-BEBOP also exhibits a reasonable degree of tolerance to values of T_2 other than the specific value used in optimizing the pulse, as shown in Fig. 8. A pulse designed for the shortest expected T_2 performs well for all longer values (although not as well as a pulse optimized specifically for the longer values).

4 Experimental

To test the performance of RC-BEBOP pulses, experimental excitation profiles analogous to the simulations shown in Fig. 2B were measured on a Bruker Avance 250 MHz spectrometer equipped with SGU units for RF control and

linearized amplifiers. A sample of 99.96% D₂O was saturated with CuSO₄ to final relaxation times at 296 K of $T_1 = 1.7$ ms and $T_2 = 0.8$ ms. A pulse of length 1 ms and maximum RF amplitude 15 kHz was optimized for these experimentally derived relaxation times, giving a similar pulse shape to the one shown in Fig. 5, optimized for $T_1 = T_2 = 1$ ms. The maximum RF amplitude was calibrated using a hard pulse and by comparing experimental with theoretically expected offset patterns of several pattern pulses [17]. Offset profiles for the optimized pulse and the hard pulse were obtained by varying the offset of the pulses from -25 kHz to 25 kHz in steps of 1 kHz. The results are shown in Fig. 9. The experimental data provide an excellent match with theory and represent a **noticeable** improvement at offsets exceeding ± 10 kHz.

5 Conclusion

We have derived an algorithm using optimal control theory to mitigate the effects of T_1 and T_2 relaxation during the application of long pulses. The procedure is quite general and has many potentially useful applications. It was applied here specifically to Broadband Excitation by Optimized Pulses (BEBOP), since we have used them routinely as a simple proxy for characterizing the performance and capabilities of optimal control in general within the context of NMR. The resulting relaxation-compensated RC-BEBOPs extend the utility of BEBOP pulses to applications in which T_1, T_2 are short compared to the pulse length. Potential applications include, e.g., ¹³C spectroscopy of proteins with paramagnetic centers. In addition, the shortest possible T_1 was shown to be advantageous for the performance of optimized pulses, due to repolarization.

Since the benchmark for performance of broadband excitation in many applications is a phase-corrected hard pulse, we also considered RC-BEBOPs which produce a linear phase roll in the excited magnetization. Designing pulses with specific phase characteristics for the final magnetization is a new approach in our optimal control work and also has many potential applications. For the demanding case of T_1 and T_2 equal to a pulse length of 1 ms, RC-BEBOP uniformly excites $\sim 99\%$ transverse magnetization over a bandwidth of 50 kHz, tolerant to $\pm 5\%$ RF inhomogeneity, with deviations of less than 2° from linear phase at the maximum inhomogeneity. Pulse performance is robust when relaxation is longer than the design values.

Acknowledgments

T.E.S. acknowledges support from NSF Grant CHE-0518174. B.L. thanks the Fonds der Chemischen Industrie and the Deutsche Forschungsgemeinschaft (Emmy Noether fellowship LU 835/1-3) for support. S.J.G. acknowledges support from the Deutsche Forschungsgemeinschaft for Grant Gl 203/4-2 and the Fonds der Chemischen Industrie.

References

- [1] T.E. Skinner, T.O. Reiss, B. Luy, N. Khaneja, S.J. Glaser, Application of optimal control theory to the design of broadband excitation pulses for high resolution NMR, *J. Magn. Reson.* 163 (2003) 8–15.
- [2] T.E. Skinner, T.O. Reiss, B. Luy, N. Khaneja, S.J. Glaser, Reducing the duration of broadband excitation pulses using optimal control with limited RF amplitude, *J. Magn. Reson.* 167 (2004) 68–74.
- [3] K. Kobzar, T.E. Skinner, N. Khaneja, S.J. Glaser, B. Luy, Exploring the limits of broadband excitation and inversion pulses, *J. Magn. Reson.* 170 (2004) 236–243.
- [4] T.E. Skinner, T.O. Reiss, B. Luy, N. Khaneja, S.J. Glaser, Tailoring the optimal control cost function to a desired output: application to minimizing phase errors in short broadband excitation pulses, *J. Magn. Reson.* 172 (2005) 17–23.
- [5] T.E. Skinner, K. Kobzar, B. Luy, M.R. Bendall, N. Khaneja, S.J. Glaser Optimal control design of constant amplitude phase-modulated pulses: Application to calibration-free broadband excitation, *J. Magn. Reson.* 179 (2006) 241–249.
- [6] P. J. Hajduk, D. A. Horita, and L. E. Lerner, Theoretical analysis of relaxation during shaped pulses. I The effects of short T_1 and T_2 , *J. Magn. Reson. Series A* 103 (1993) 40–52.
- [7] J.-M. Nuzillard and R. Freeman, Band-selective pulse designed to accommodate relaxation, *J. Magn. Reson.* 107 (1994) 113–118.
- [8] D.E. Rourke, L. Khodarinova, and A.A. Karabanov, Two-Level Systems with Relaxation, *Phys. Rev. Letters*, 92 (2004), 163003(1–4).
- [9] D. E. Rourke, A. A. Karabanov, G. H. Booth, and I. Frantsuzov, The Bloch equation when $T_1 = T_2$, *Inverse Problems*, 23 (2007), 609–623.
- [10] S. Conolly, D. Nishimura, A. Macovski, Optimal control solutions to the magnetic resonance selective excitation problem, *IEEE Trans. Med. Imaging* MI-5 (1986) 106–115.

- [11] J. Mao, T.H. Mareci, K.N. Scott, E.R. Andrew, Selective inversion radiofrequency pulses by optimal control, *J. Magn. Reson.* 70 (1986) 310–318.
- [12] D. Rosenfeld, Y. Zur, Design of adiabatic selective pulses using optimal control theory, *Magn. Reson. Med.* 36 (1996) 401–409.
- [13] M. H. Levitt and L. DiBari, Homogeneous master equation and manipulation of relaxation networks, *Bull. Magn.Reson.* 16 (1994) 94–114.
- [14] N. Khaneja, T. Reiss, C. Kehlet, T. Schulte-Herbrüggen, and S.J. Glaser, Optimal control of coupled spin dynamics: design of NMR pulse sequences by gradient ascent algorithms, *J. Magn. Reson.* 172 (2005) 296–305.
- [15] A. J. Shaka and A. J. Pines, Symmetric phase-alternating composite pulses, *J. Magn. Reson.* 71 (1987) 495-503.
- [16] E. Kupče and R. Freeman, Wideband excitation with polychromatic pulses, *J. Magn. Reson.* 108 (1994), 268–273.
- [17] K. Kobzar, B. Luy, N. Khaneja, S. J. Glaser, Pattern pulses: design of arbitrary excitation profiles as a function of pulse amplitude and offset, *J. Magn. Reson.* 173, (2005) 229–235.

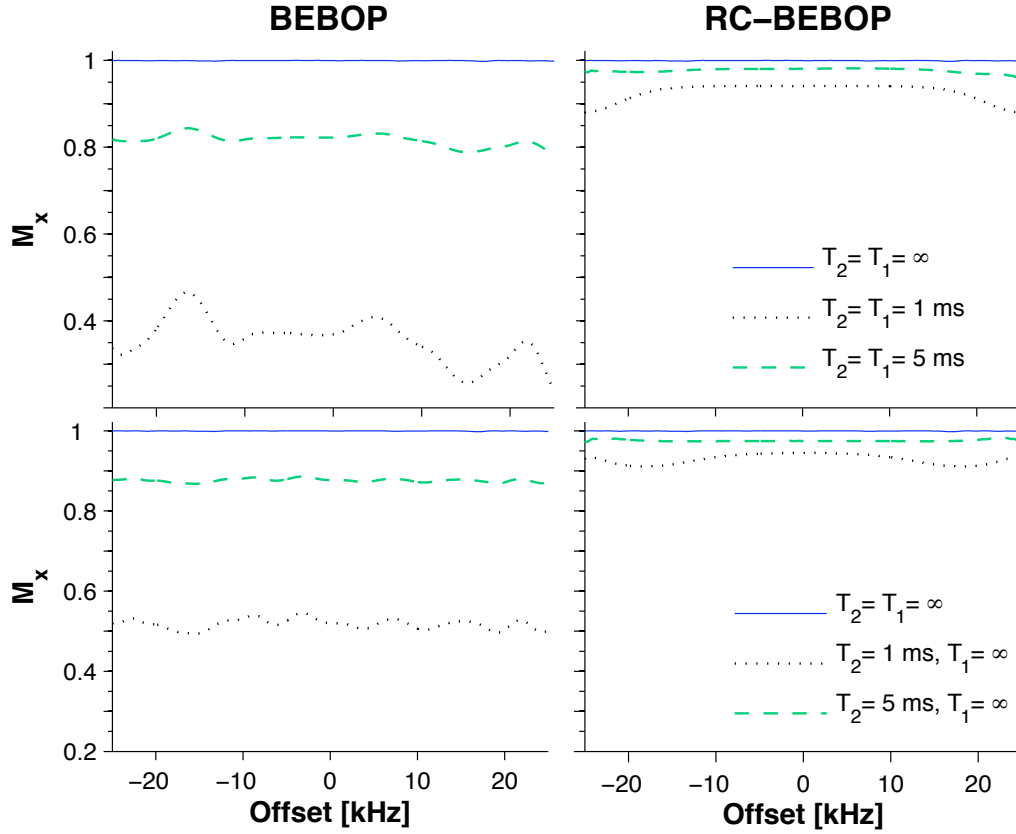


Fig. 1. Simulated performance of the phase-modulated BEBOP from Ref. [5] (left panel) and corresponding relaxation-compensated RC-BEBOP pulses (right panel) for the T_1 and T_2 values listed on the right. The length of both pulses is 1 ms. The M_x -component of magnetization is plotted as a function of resonance offset, with the nearly perfect performance of the pulses in the absence of relaxation illustrated by the solid blue line at the top of each figure. PM-BEBOP performance is significantly degraded for short T_2 (bottom panels) and short $T_2 = T_1$ (top panels), while RC-BEBOP achieves performance comparable to the case of no relaxation.

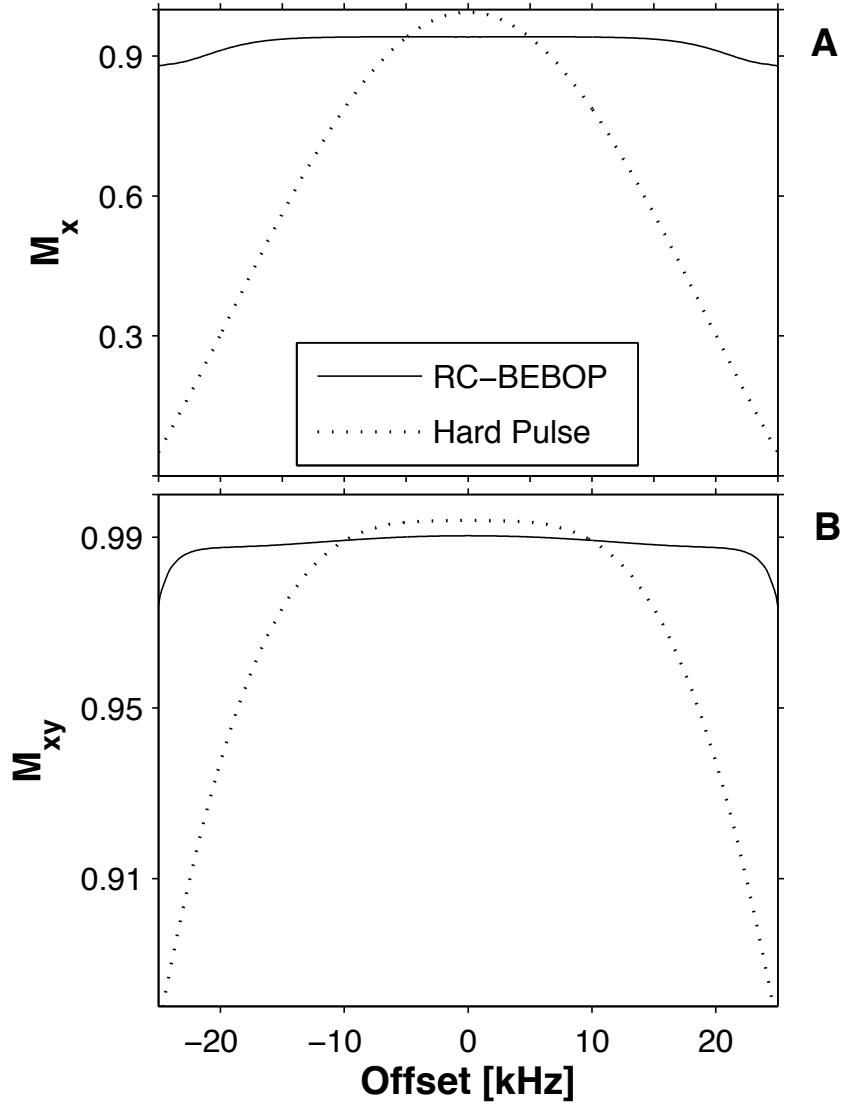


Fig. 2. RC-BEBOP performance compared to a hard pulse for relaxation times $T_2=T_1=1$ ms equal to the RC-BEBOP pulse length. The maximum RF amplitude of all pulses is 15 kHz ($16.7 \mu\text{s}$ hard pulse). Note the change in scale between the two plots. **(A)** M_x components of the magnetization resulting from application of a hard pulse and RC-BEBOP designed to produce minimal phase dispersion are plotted as a function of resonance offset. **(B)** transverse M_{xy} is plotted for a separate RC-BEBOP designed to allow a linear phase roll in the final spectrum and is compared to the performance of a hard pulse. Despite conditions for potentially severe relaxation, RC-BEBOP uniformly excites $\sim 99\%$ of the transverse magnetization over a bandwidth of almost 50 kHz.

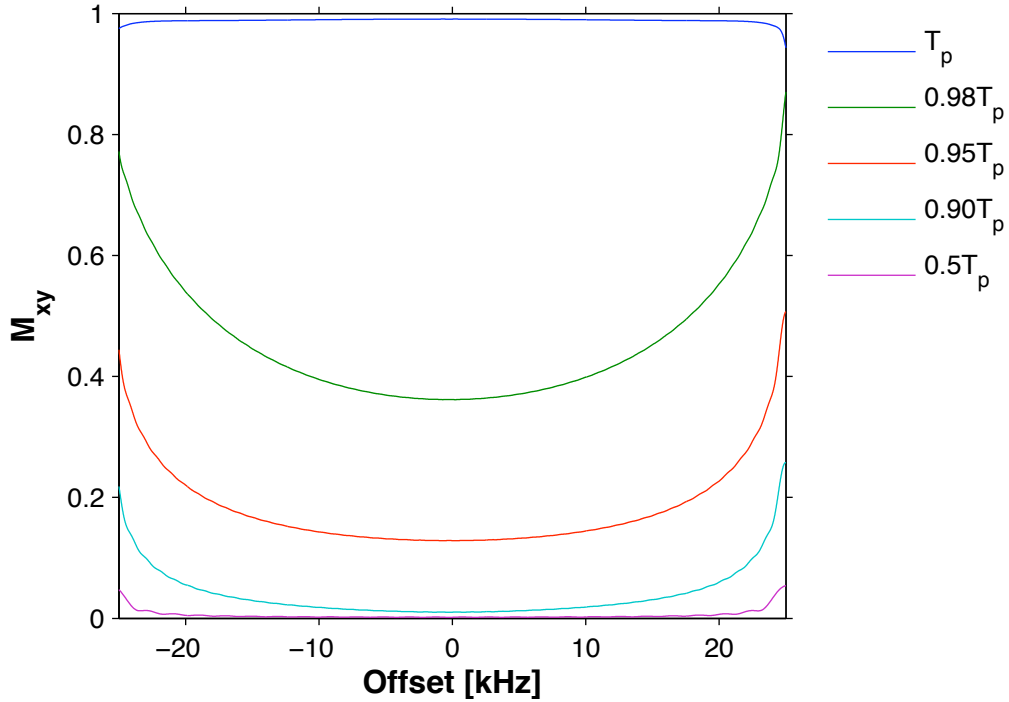


Fig. 3. The transverse magnetization $M_{xy}(t)$ resulting from application of the linear phase RC-BEBOP of Fig. 2B is plotted as a function of resonance offset at the times shown in the figure legend. Spins at all offsets stay very close to the z -axis ($\sqrt{1 - M_{xy}^2} > 0.87$) during the first 95% of the pulse, with spins at the extremes of the bandwidth having been rotated the farthest from z at each time. Relaxation effects are thus minimized by positioning spins of each offset at the proper orientation near the z -axis that allows all offsets to be transformed to the transverse plane by what amounts to a hard pulse (see Fig. 5A) during the final 2% of the pulse length.

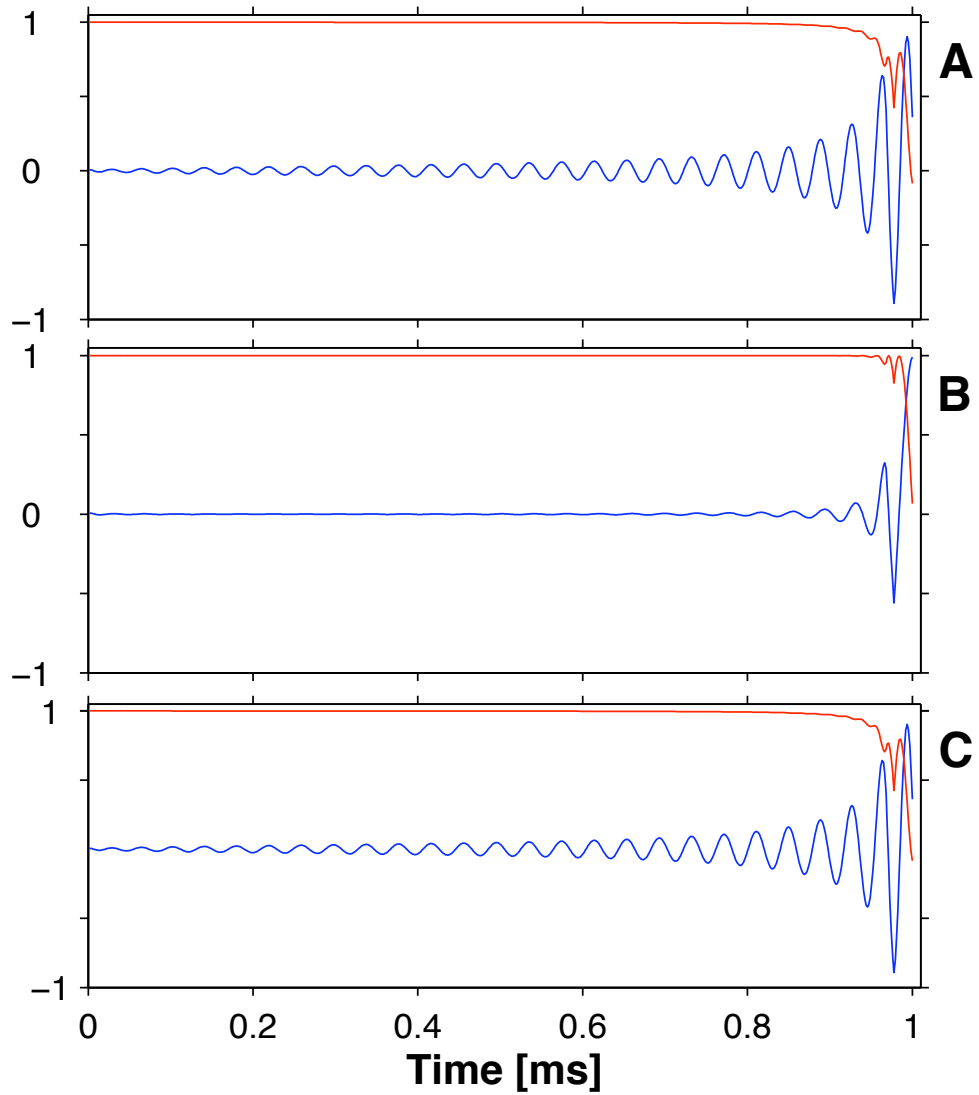


Fig. 4. The M_z (red) and M_x (blue) components of magnetization resulting from application of the linear phase RC-BEBOP of Fig. 2B are plotted as a function of time for resonance offsets (A) -25 kHz, (B) 0 kHz, and (C) 25 kHz. The pulse mitigates relaxation effects by positioning spins of each offset at the proper orientation near the z -axis that allows all offsets to be transformed to the transverse plane in a relatively short time at the end of the pulse.

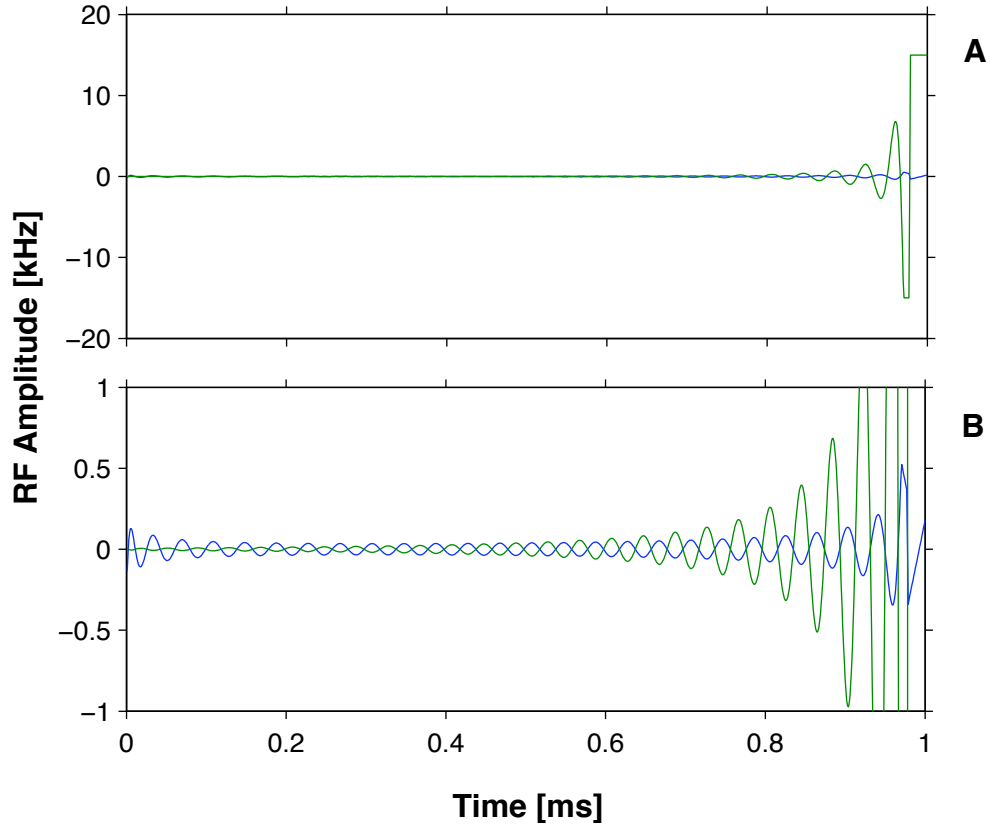


Fig. 5. RC-BEBOP pulse of Fig. 2B plotted as a function of time. (A) RF amplitude plotted as x -phase (blue) and y -phase (green). The small, but nonzero, amplitude for $\sim 80\%$ of the pulse length, shown more clearly in (B), affects primarily the extremes of the bandwidth, as demonstrated in Fig. 3 and discussed in the text. Once the spins at each offset are oriented properly during $\sim 0.98T_p$, a hard pulse at the very end transforms all the spins to transverse M_{xy} with linear phase as a function of offset. Deviations from linearity are less than 0.3° for the ideally calibrated pulse, with deviations less than 2° for RF inhomogeneity/miscalibration of $\pm 5\%$.

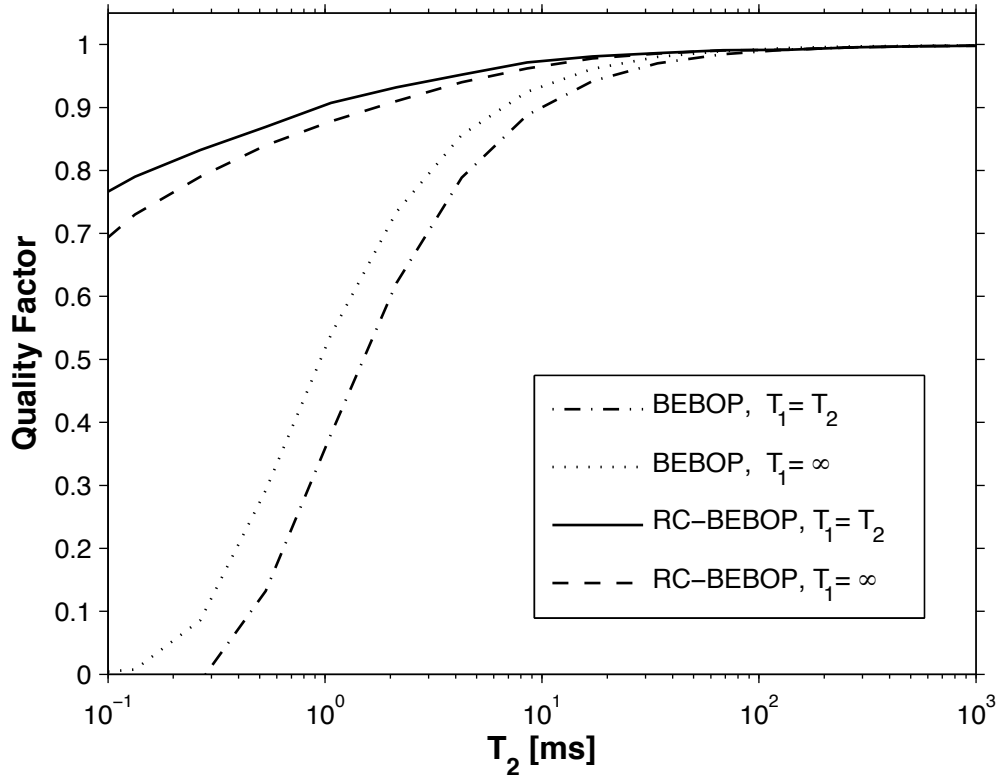


Fig. 6. The quality factor, QF, measuring how well the pulse achieves a target magnetization M_x over the range of resonance offsets and RF inhomogeneity, is plotted for PM-BEBOP and RC-BEBOP as a function of T_2 . Each point on a curve represents the performance of the corresponding pulse for the associated value of T_2 given on the graph and the value of T_1 shown in the figure legend. RC-BEBOP was designed specifically for these values at each point. In contrast to a long pulse with no compensation for relaxation effects, short T_1 results in improved performance for RC-BEBOP.

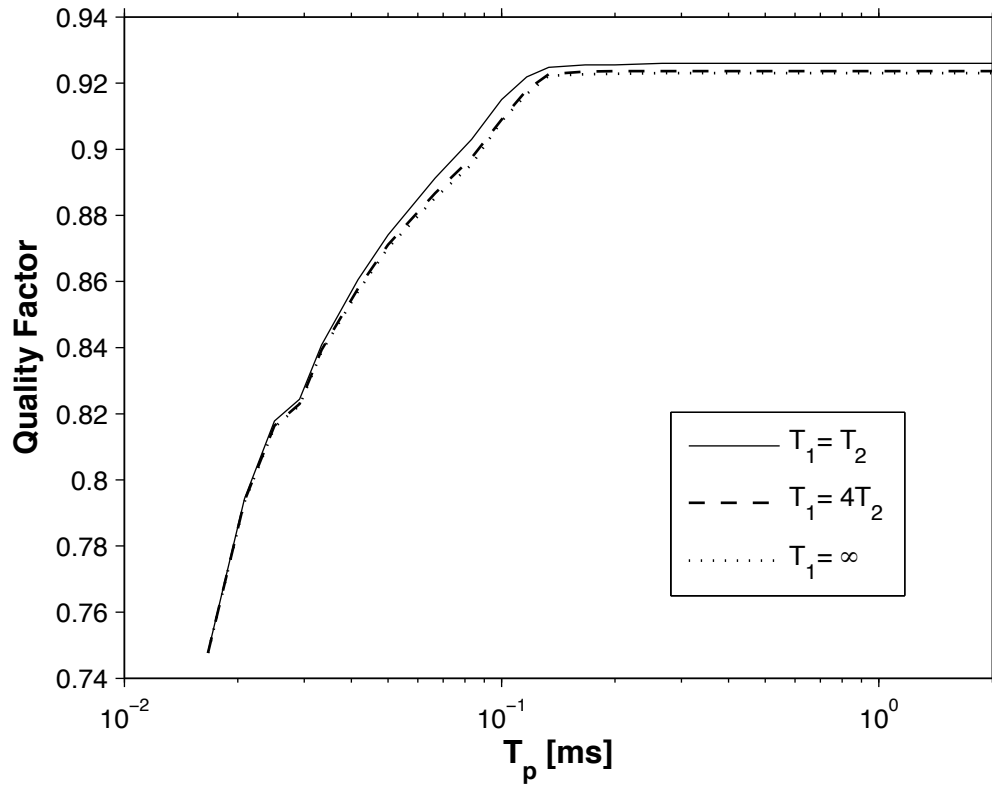


Fig. 7. Quality factor of RC-BEBOP as a function of pulse length for values of the ratio T_2/T_1 in the range $[0,1]$ for $T_2 = 1$ ms. Performance design parameters are similar to Fig. 6, but with a smaller tolerance to RF miscalibration of $\pm 5\%$. The quality factor obtainable with RC-BEBOP is relatively insensitive to T_1 for values of T_2 greater than 1 ms (see, also, Fig. 6).

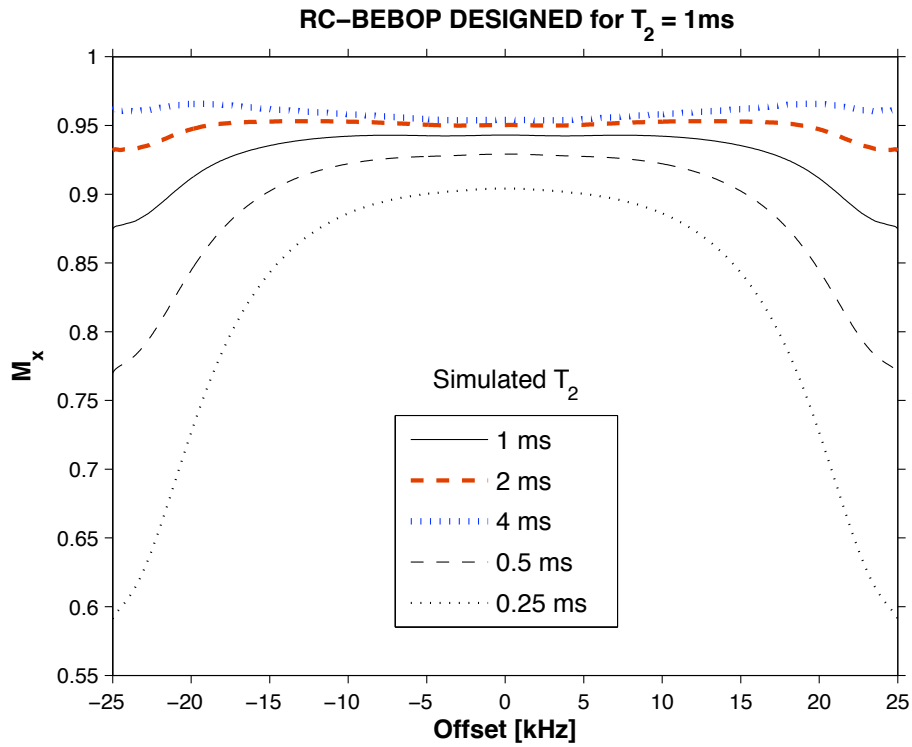


Fig. 8. Performance of RC-BEBOP designed for $T_1 = T_2 = 1\text{ ms} = t_p$. The M_x -component of magnetization is plotted as a function of resonance offset for the operative T_2 values listed in the figure legend. Pulse performance is somewhat degraded if actual T_2 values are less than the design value, but larger T_2 values are advantageous.

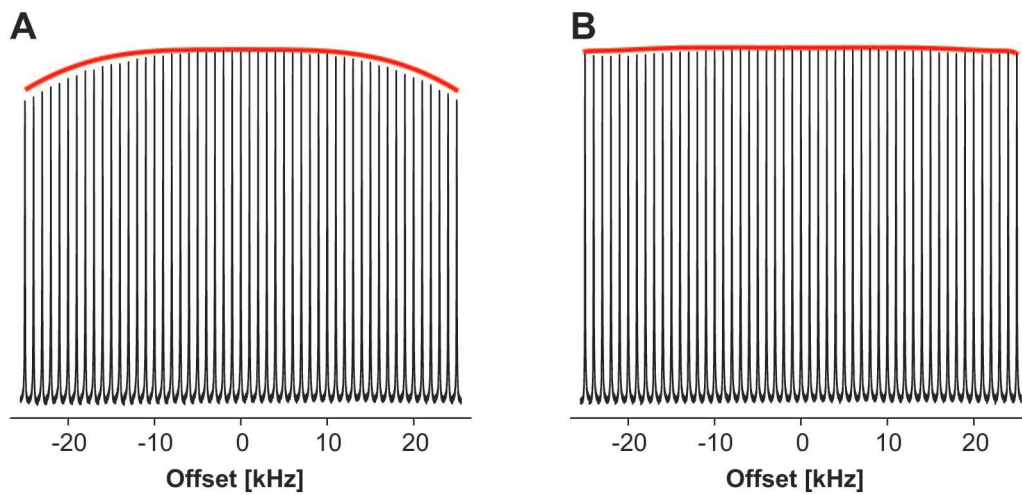


Fig. 9. Experimental performance analogous to the simulations of Fig. 2B for **(A)** a hard pulse and **(B)** RC-BEBOP optimized for the measured sample relaxation times $T_1 = 1.7$ ms and $T_2 = 0.8$ ms. All other parameters are the same as for the simulations. Further details can be found in the Experimental section.